Influence of a Realistic Loading on Characteristics and Design of ESPAR

Albert A. Lysko[1] and Mofolo Mofolo[1,2]
CSIR Meraka Institute
Council for Scientific and Industrial Research[1]
PO Box 395, Pretoria 0001, South Africa
Tel: +27 12 841 4609, Fax: +27 12 841 4720
email: alysko@csir.co.za
and Department of Electrical and Electronic Engineering Sciences
Faculty of Engineering and the Built Environment
University of Johannesburg[2], Johannesburg, South Africa

Abstract-The paper presents results of a study considering a 2.4 GHz low-cost low-power-consumption electronically switched parasitic array radiator (ESPAR) antenna suitable for wireless sensor networks and rural applications. The paper discuses the effects of realistic versus ideal loads in the process of modeling and design on the example of a four plus one elements antenna. The realistic loading is found to have a significant effect on the design, e.g. reducing the gain by over 2 dB and the return loss by up to 6 dB. The paper presents several optimized designs, offering gain of 9 dBi and excellent impedance match.

Index Terms—parasitic arrays, antenna, ESPAR, loading, antenna design

I. INTRODUCTION

Parasitic array antennas normally require less semiconductor elements for beam control, are typically less complex to manufacture, and have lower cost than the usual phased arrays, yet offer most of their benefits. This makes the parasitic arrays an attractive choice for budget sensitive applications like wireless sensor networks (WSN) and communication for rural undeserved areas of Africa.

A parasitic array antenna usually includes one active element and several parasitic elements. The active element is connected to a radio frequency (RF) waveguide. The parasitic elements are used to capture the electromagnetic waves incident upon them and to re-radiate them, serving to focus the beam. A basic example of a parasitic array antenna is Yagi antenna [1] that has an active half-wavelength dipole, reflector and directors. The reflector is a parasitic element slightly longer than the active element and which reflects the waves back towards the active element. The directors are shorter than the active element and help to guide the radiation in one direction.

An electronically switched parasitic array radiator (ESPAR) antenna [2-5, 8] has electronically controllable loads terminating the parasitic elements as demonstrated in Fig. 1. This provides the means to control the function of the parasitic elements, e.g. to perform as a reflector or director.

In order to *steer* the beam, the load requires a fine control. Usually, this is done by using a varactor controlled by a digital-to- analog converter (ADC). Our application is cost and power consumption sensitive, thus this choice did not seem optimal. *Switching* the beam between a sufficient number of different directions can require much simpler and less power hungry circuitry and is the direction chosen in this work. In our case, each load can be switched between two states. In principle, it is possible to switch between open-circuit, short-circuit, inductive and capacitive loads. In this work, only the open and short circuiting loads were considered.

Most of the research papers on ESPAR known to the author are based on the idealized loads. This paper considers and discusses some of the effects of realistic loads on the gain and input impedance of a 2.4 GHz band ESPAR

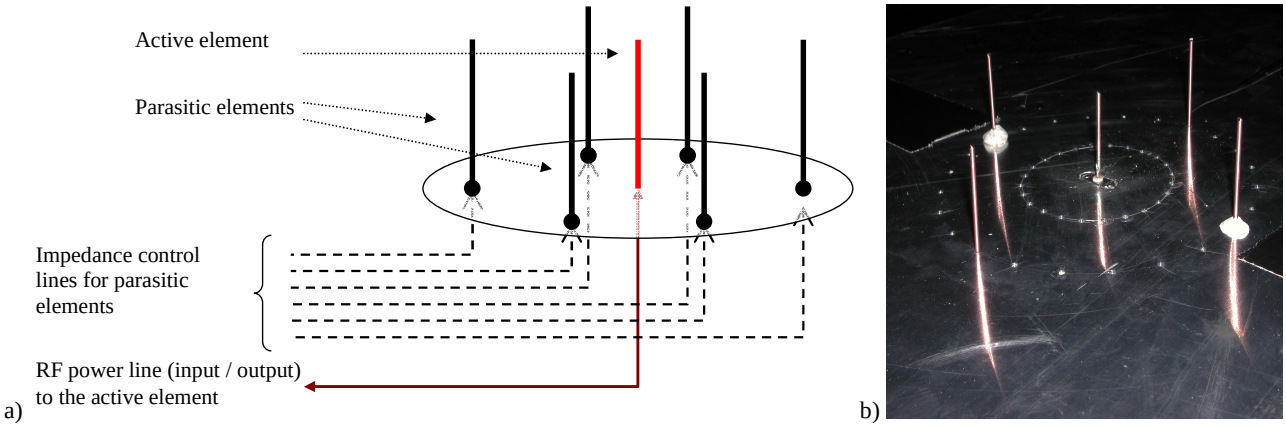

Fig. 1. a) Schematic view of an electronically switched parasitic array radiator (ESPAR) antenna. b) Prototype.

antenna. The focus on four parasitic elements was for the sake of simplicity and length of the paper.

The paper is organized as follows. Section II introduces tools, approximations and notations and optimization criteria used later in the text. Section III discusses the cases studied and the results. The last section concludes the paper.

II. Methodology, Approximations, Results and Discussions

To perform the full wave electromagnetic modeling, this work relies on the numerical modeling tool WIPL-D v.6.0 Lite [6]. The model of a parasitic array antenna was build using wire model [7]. The accuracy of modeling by the tool has been verified by building a prototype shown in Fig. 1b, and performing radiation pattern measurements in an anechoic chamber. The results of the measurements matched the results of the modeling very well [4, 5].

The antenna is modeled as an array of monopoles on an infinite ground plane. The array has one central active/fed element of height H_a, and four parasitic elements with height H_p placed uniformly around a circle of radius R with the centre at the active element. Wire radius of 1 mm was used for all elements in all models in this paper. In all models, it is also assumed that each parasitic element is terminated in a load which may be switched between only two states (e.g. an open-circuit high-impedance state and closed-circuit low-impedance state). In all models, the two neighboring parasitic elements have the same load and the remaining opposing two parasitic elements are in the other/opposite state, as to obtain a strong single main beam [8]. The parasitic monopoles of ESPAR are assumed to be loaded via a single pole dual throw (SPDT) radio frequency (RF) switch. Both ideal and non-ideal models of the switch are considered. An idealized SPDT switch is assumed to be located on the top of the ground plane, i.e. on the same side as the parasitic monopole elements, as per Fig. 1b.

The model of non-ideal SPDT switch used in this work is based on Infineon BGS12AL7-6. The latter connects the RF signal from RFin to either RF1 or RF2 – the notations are as per the datasheet [9]. The scattering matrix data for the switch was imported into WIPL-D and then used to create the model as shown in Fig. 2. Ports 1, 2 and 3 of the model correspond to the ports RFin, RF1 and RF2, respectively.

Optimization functionality built into WIPL-D [6] was used to tune the geometry of the antenna, via the parameters R, H_p and H_a. As WIPL-D's Lite version permits only 2 optimization variables, the weights per each condition were varied before changing the optimization variables between R, H_p and H_a manually, and re-starting the optimization runs. The following optimization criteria were used:

1) Maximum gain to be above 15 dBi;
2) Side lobes to be below 0 dBi;
3) Real part of the input impedance to be greater than 10 Ohm / equal 50 Ohm (both cases were used);
4) Imaginary part of the input impedance to be less than 10 Ohm / equal 0 Ohm (both cases were used).

The modeling was done in several stages. First, an ideal switch was assumed, shown as the cases #0a and 0b in Table 1. The results are shown as the blue curves in Fig. 3 and configurations A and C in Table 2. It is clear that the ideal loads offer the highest gain and a reasonable impedance match. For example, the input impedance of the configuration C may be matched to the standard 50 Ohm port using a method from [10].

Table 1. Equivalent input impedance of the RF switch at port 1, Z_{equiv}, when the other two ports are connected to various terminating loads shown in the second column (ports are denoted with letter P and numbers, and the state is shown as follows: *O* is an ideal open circuit, *S* is an ideal short circuit, *L* is a via characterized as an impedance of 0.08 Ohm and 1.34 nH connected in series to the ground, *C* is an open microstrip line with equivalent impedance of the series connection of 0.93 Ohm and 0.28 pF connected in series to the ground, *L2* and *C2* are the same as *L* and *C* except for the increase of values to 2 nH and 0.4 pF, respectively)

Case #	Switch termination scenario	Z_{equiv}, Ohm	Switch state
0a	No switch (ideal load)	0 (used 0.01Ω)	On (SC)
0b	No switch (ideal load)	+∞ (used 5kΩ)	Off (OC)
1	Ideal1: P2=*S*,P3=*O*	3.5 + j19.5	On (SC)
2	Ideal2: P2=*O*,P3=*S*	2.8 – j60.4	Off (OC)
3	Non-ideal: P2=*L*, P3=*C*	8.6 + j61.7	On (SC)
4	Non-ideal: P2=*C*, P3=*L*	2.45 – j42.7	Off (OC)
5	Non-ideal: P2=*L2*, P3=*C2*	17.5 + j104.6	On (SC)
6	Non-ideal: P2=*C2*, P3=*L2*	2.42 – j37.5	Off (OC)

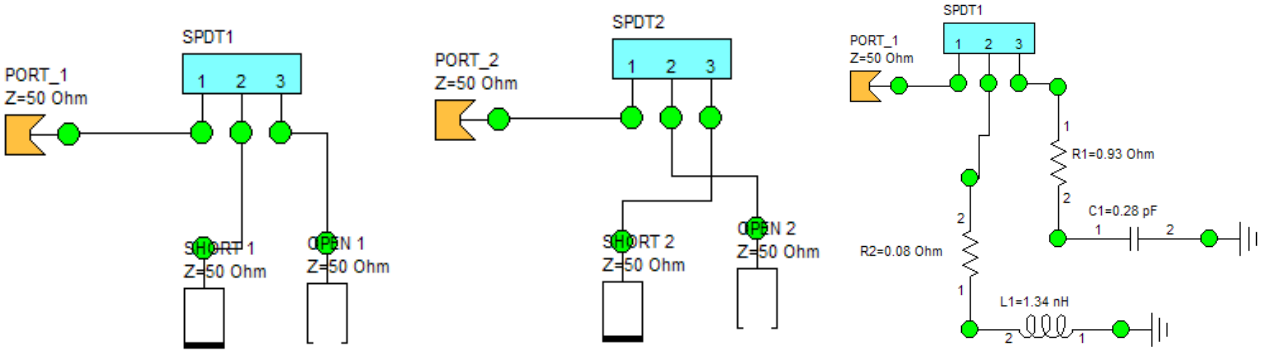

(a) (b) (c)

Fig. 2. Three samples of various non-ideal loading models: (a), (b) non-ideal switch terminated by the ideal open and short circuits, (c) non-ideal switch terminated by a short circuit (a via, i.e. inductor) and an open circuit (capacitor).

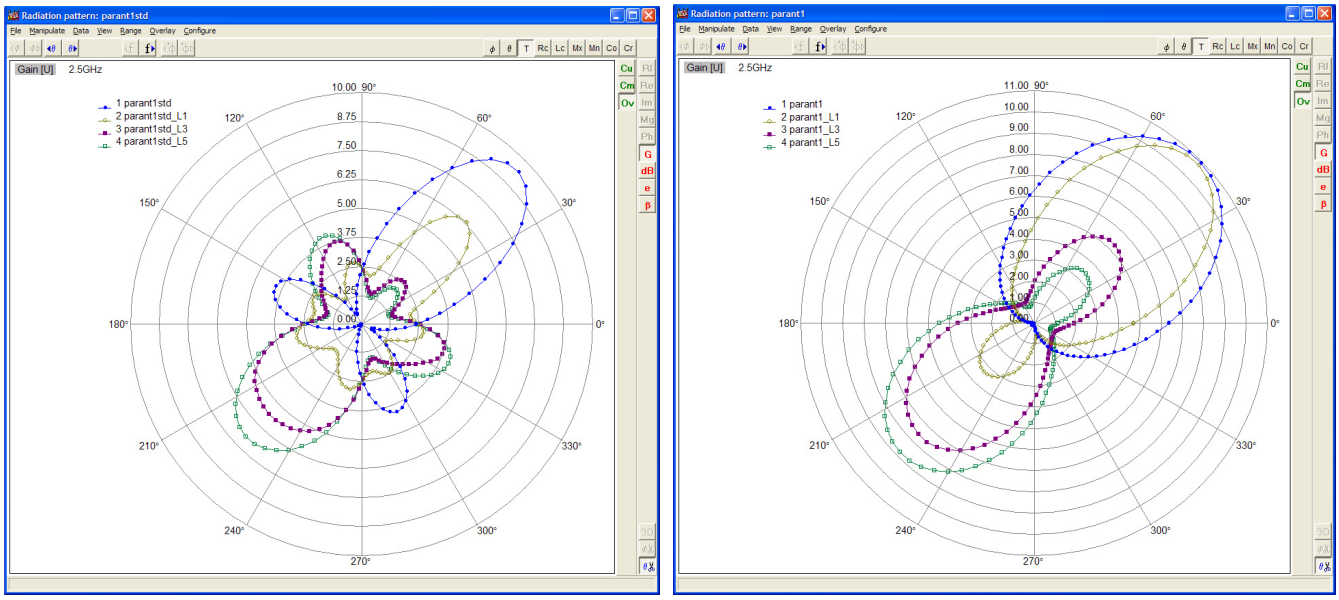

(a) (b)

Fig. 3. Power gain patterns for ideal and realistic load models for a standard (a) and optimized (b) geometries. Legend entries with *L1*, *L3*, and *L5* correspond to the loading cases #1, 3 and 5 from Table 1, respectively.

Next, the non-ideal models, i.e. the models including losses and delay, were tested. In an ideal case, the parasitic element is connected directly to the ground plane, with no losses or delays. In reality, the finite size of the load, composed of a switch, its termination, and interconnecting transmission lines, together with the losses in the switch and non-ideal termination, cause change in both phase and amplitude of the reflection coefficient. In order to model the non-ideal switch, the scattering matrix parameters of the switch were obtained [9] and used in the microwave circuit simulator WIPL-D Microwave [6].

The non-ideal switch, connected to an ideal open and short circuits, converts these ideal states into the states with equivalent impedance of +j19.5 Ohm and –j60.4 Ohm, as shown with the cases 1 and 2 in Table 1. This differs from zero and infinity Ohms of an ideal termination of a parasitic element in both magnitude and phase, and was thus expected to degrade the performance of a non-optimized array. As a confirmation, Fig. 2 shows that such introduction of the realistic loading changes the radiation patterns drastically, not just reducing the maximum gain but also affecting the direction of the main beam (easily seen for the geometries L3 and L5).

Table 2 shows an overview of the key results. The initial idealistic setup was based on the most common half/quarter wavelength distance array recipe indicated by the configuration A. Later, its geometry was optimized to obtain a higher gain, shown in the configuration/design C. The value of the highest gain of 10.39 dBi can be used as a figure of merit. It may also be noted that the value of the input impedance was significantly reduced, as the result of stronger coupling to the ground through the parasitic elements, which are here much closer to the active element.

Next, the realistic models for the loads were added to the design. Fig. 4 shows gain patterns for these new designs. The addition of realistic loads including effects of losses and delays brought the performance of the initial design A significantly down. The gain was reduced by over 2 dB, whilst the level of the side lobes rises to nearly reach the level of the main lobe (the effect is especially strongly pronounced in the configuration B). Addition of the realistic loads caused even greater problem with the optimized design C. Its performance was reduced, as can be observed from the performance of the configuration D. In comparison to C, the configuration D has lost nearly 2 dB in terms of gain and over 6 dB in terms of the return loss, making the return loss as low as 3 dB.

Following these observations, the design D was optimized, using various combinations of weights per each optimization criterion. The geometrical parameters and the

Table 2. Geometry and performance parameters for several configurations.

Load and antenna configuration #	**Name in Fig. 3 with radiation patterns (*parant1*+…)**	**Ha, mm**	**Hp, mm**	**R, mm**	**Input impedance of antenna Z_{in}, Ohm**	**Max gain G_{max}, dBi**	**SLL, dB**
A. *Idealistic* load	std	28	28	60	42.3 – j20.4 (RL= 12dB)	9.75	3.65
B. Realistic load	std_L3	28	28	60	44.9 – j10.6 (RL=18dB)	7.43	1.68
C. *Idealistic* load		26.21	32.7	26.51	24.5 – j1.29 (RL=9dB)	10.39	18.39
D. Realistic load	_L3	26.21	32.7	26.51	8.8 + j 9.07 (RL=3dB)	8.78	1.98
E. Realistic load	_L3_opt	24.96	35.26	26.39	9.0 – j0.3 (RL=3.1dB)	9.39	7.14
F. Realistic load	_L3_opt_A	26.21	33.4	40.41	72.4 + j12.1 (RL=13.7dB)	9.05	5.81
G. Realistic load	_L3_opt1	24.96	34.13	38.77	56.1 + j5.9 (RL=22dB)	9.06	7.06

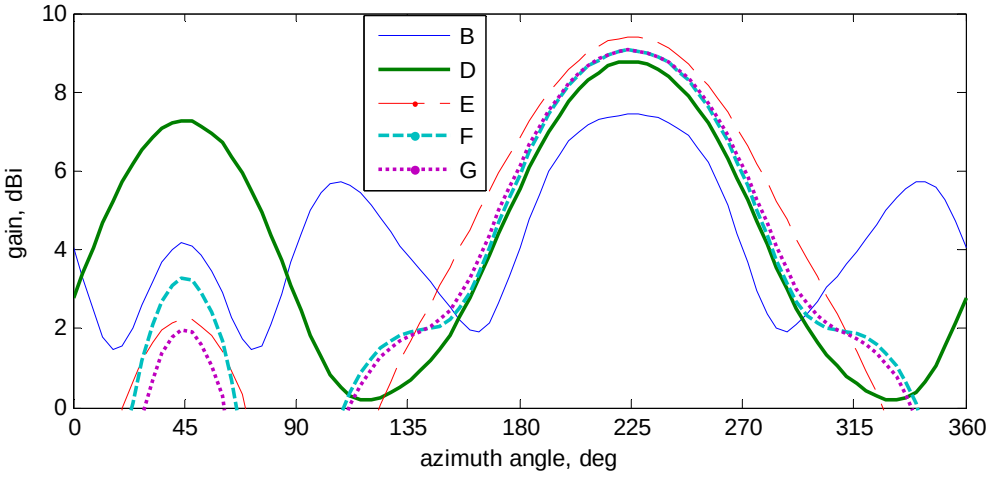

Fig. 4. Gain pattern for various configurations named in accordance to the first column of Table 2.

performance results are shown as designs E, F, and G in Table 2 and Fig 4. These designs show similar performance in terms of the gain, a slight difference between E, and G against F in terms of the side lobe level (SLL), and a large difference in terms of the input impedance. The design E has very low input impedance, which nevertheless is real and could be matched using, for example, a quarter-wave transformer [10] with line impedance of 21.2 Ohm. This transformer could in practice introduce a small loss of under 0.15 dB. The designs F and G do not require any additional impedance matching circuitry, for most practical applications. Out of the two designs, the latter is expected to provide a slightly better performance, due to both lower side lobes and better impedance matching.

III. Summary

An electronically switched parasitic array with four parasitic elements has been modeled assuming a non-ideal RF switch. The model of the switch was based on a combination of the measured data and simulation models. It was found that neglecting to include the realistic model may lead to a large error in maximum gain or even incorrect prediction for the direction of the main beam. Moreover, it was found that the non-ideal load may reduce the return loss by as much as 6 dB and possibly more.

An improved series of designs proposed in the paper display better than 9 dB gain, better than 7 dB side lobe level, and several possible values for the input impedance, including one providing the return loss value of better than 22 dB at a 50 Ohm port.

IV. References

1. J. D. Kraus and R. J. Marhefka, *Antennas*, McGraw-Hill, 2001.
2. R. F. Harrington, "Reactively Controlled Directive Arrays," *IEEE Trans. Antennas Propagat.*, Vol. AP-26, May 1978, pp. 390–395.
3. T. Ohira and K. Iigusa, "Electronically Steerable Parasitic Array Radiator Antenna," *Electronics and Communications in Japan*, Part 2, Vol. 87, No. 10, 2004, pp. 25-45.
4. M. Mofolo, A. A. Lysko, and W. Clarke, "A Method of Electronic Beam Steering For Circular Switched Parasitic Dipole Arrays." *Southern Africa Telecommunication Networks and Applications Conference (SATNAC)*, Spier Estate, Stellenbosch, South Africa, 5-8 September 2010, 6 pages.
5. M. Mofolo, A. A. Lysko, and W. Clark, "Beam Steering for Circular Switched Parasitic Arrays Using Combinational Approach." Submitted for *IEEE Africon 2011*, Zambia, Sept 2011, 6 pages. In Press.
6. B. M. Kolundzija, J. S. Ognjanovic, and T. K. Sarkar, *WIPL-D Microwave: Circuit and 3D EM Simulation for RF & Microwave Applications - Software and User's Manual*, Artech House, 2006, 400 pages.
7. B. M. Kolundzija and A. R. Djordjevic, *Electromagnetic Modeling of Composite Metallic and Dielectric Structures*, Artech House, 2002.
8. R. O. M. Mofolo, *Enhanced Beam Steering and Parameter Analyses for Switched Parasitic Arrays*, draft of Masters thesis, Johannesburg University, 2011, 146 pages.
9. *BGS12AL7-6 SPDT RF Switch Datasheet*, Revision 2.0, Infineon Technologies AG, Germany, 2009, 16 p.
10. D. M. Pozar, *Microwave Engineering*, 3rd Ed., Willey, 2004, 720 pages.

Dr Albert Lysko is with the CSIR Meraka Institute. He is a Senior Member of IEEE, reviewer for IEEE journals and conferences, has published over two dozen papers. His research interests include smart antennas, wave propagation, wireless networking and spectrum management and cognitive radio.